HortScience 58(12):1488–1491. 2023. https://doi.org/10.21273/HORTSCI16961-22

Abnormal Pollen Development in the *Fragaria vesca* Mutant *fruitless 1*

Janet P. Slovin and Laura E. Dougherty

Genetic Improvement of Fruits and Vegetables Laboratory, US Department of Agriculture, Agricultural Research Service (USDA-ARS), BARC-W 10300 Baltimore Avenue, Beltsville, MD 20705, USA

Keywords. anther, diploid strawberry, ethyl methanesulfonate mutagenesis, microscopy, sexual reproduction, single gene

Abstract. **Knowledge of the genes underlying a given trait is highly useful for developing molecular markers for breeding and is the foundation for future genomic crop improvements. The cultivated strawberry, *F.* ×*ananassa*, is a valuable horticultural crop. Genome sequencing revealed that of the four diploid strawberry subgenomes contributing to the *F.* ×*ananassa* octoploid genome, the woodland strawberry, *F. vesca*, subgenome is dominant. Thus, *F. vesca* is an important system for determining gene function and should be used as a source of genetic diversity for *F.* ×*ananassa* breeding. Ethyl methanesulfonate mutagenesis of H4 F7-3, an inbred line of *F. vesca*, resulted in one M2 line that did not produce any strawberries over a 3-year period in the greenhouse. This line was named *fruitless 1*. The *fruitless 1* phenotype results from a single gene recessive mutation. Microscopic characterization revealed that *fruitless 1* failed to produce fruit because anthers fail to develop properly before meiosis, resulting in no pollen production. This report of *fruitless 1* facilitates further studies of the line.**

Mutants have played a critical role in identifying genes regulating specific traits, thus elucidating their function in *Arabidopsis*, which is a noncrop plant that is a reference plant for genomics in many crops (Cao et al. 2021; Kuo et al. 2021). The diploid woodland strawberry *Fragaria vesca*, like Arabidopsis, has many characteristics that make it amenable to experimentation (Slovin and Rabinowicz 2007; Slovin et al. 2009). *F. vesca* is a small perennial that bears a highly aromatic and edible organ commonly called a berry. A high-quality genome sequence is available for several *F. vesca* lines, including the *F. vesca* inbred line H4F7-3 (Edger et al. 2018). Of the four diploid strawberry subgenomes found in the octoploid dessert strawberry *F.* ×*ananassa*, the *F. vesca* genome appears to be dominant (Edger et al. 2019). *F.* ×*ananassa* is a high-value commodity, thus making the identification of genes that regulate growth and development invaluable. Gene sequence information is useful for marker-assisted breeding and potential genomic manipulation to improve crop production and quality.

Several naturally occurring mutants of *F. vesca* have been described. One of these, a runnerless recessive mutant (*r*) (Brown and Wareing 1965) that maps to linkage group II (Sargent et al. 2004), has been observed in nature for hundreds of years (Duchesne 1766). The causal mutation in these plants was found in the gene encoding a gibberellin 20-oxidase, which is involved in the gibberellin biosynthesis required for runner production and elongation (Tenreira et al. 2017).

Another naturally occurring mutant was found by Staudt (1959) in the progeny of a nonrunnering plant collected in the wild in Madiera. This mutant had a highly elongated crown and produced runners at every node. The mutant was named *arborea*, and it was further characterized by Guttridge (1973) as a recessive mutation that affects gibberellin synthesis in the stem internodes. A phenocopy of this mutant was found among the M2 progeny of N-ethyl-N-nitrosourea-treated *F. vesca* seeds and called *suppressor of runnerless*. This N-ethyl-N-nitrosourea-induced mutation resulted in a defective DELLA transcription factor (Caruana et al. 2018; Li et al. 2018). Other chemically induced *F. vesca* mutants exhibit round fruit shape (Wang et al. 2017), abnormal runner and stamen formation (Feng et al. 2021), less anthocyanin in petioles (Luo et al. 2018), or abnormal flower and fruit development (Pi et al. 2021). The mutated genes were identified in the latter three cases using a bulked sequencing analysis.

The M2 generation of plants from ethyl methanesulfonate (EMS) mutagenized seeds of *F. vesca* H4F7-3 were screened for plants with mutations affecting runnering and crown architecture, fruit shape, and sexual reproductive development. Four M2 plants that appeared normal except that they produced no, or very few, seeds over a 3-year period were further examined for pollen production. One of these plants, *fruitless 1* (*ftl 1*), never produced fruit and is further described here. The phenotype results from a recessive single gene mutation. Although early anther development appears to be normal, microscopic examination revealed that anther and pollen development are abnormal at the tetrad stage, and microspores degenerate during the later stages of anther development.

Materials and Methods

Plant material and growth conditions. Plants of *F. vesca* L. subsp. *vesca* forma *semperflorens* (Duchesne) Staudt inbred line Hawaii4 F7-3 (H4F7-3, PI664444) and EMS mutants were grown in controlled environment chambers under a 14-h daylength with ~150 $\mu M \cdot m^{-2} \cdot s^{-1}$ of cool white fluorescent bulbs. Growth chambers were maintained at 20 °C during the night, with an increase to 25 °C over the course of 2 h after the onset of light. Chambers were maintained at 25 °C until the lights were turned off, when the temperature was reduced to 20 °C over the course of 1 h. Plants were reproduced vegetatively by separating branch crowns and rooting these in an intermittent mist bench to produce clonal plants for experiments. Plants were also vegetatively clonally reproduced by pegging runners to moist soil with hairpins. These plants were maintained in the greenhouse under ambient conditions with supplemental light from sodium halide lamps to provide 14 h of light; then, they were moved to the growth chambers 2 weeks before sampling. Plants were grown in 10.2-cm plastic pots in a soilless mixture (2:1:1) of ProMix BX, ProMix BK25, and horticultural grade vermiculite (Whitemore Co. Inc., Lawrence, MA, USA) supplemented with dolomitic lime. Growth chamber plants were watered daily with a dilute solution of Miracle Grow™ Tomato Plant Food (Scotts Miracle-Gro Products, Inc., Marysville, OH, USA). Greenhouse-grown plants were watered with tap water and fertilized weekly with Miracle Grow™ Tomato Plant Food (Scotts Miracle-Gro Products, Inc.) according to the manufacturer's specifications.

Mutagenesis. Seeds from the inbred wild-type, H4F7-3, were imbibed and surface-sterilized as described (Rivarola et al. 2011); then, they were treated with a 0.4% solution of EMS in water for 4 h, followed by five rinses with sterile distilled water. Seeds were aseptically plated on 0.5× Murashige and Skoog salts solidified with 0.7% Phytagar (Invitrogen/ThermoFisher, Waltham, MA, USA), and the plates were placed at 6 °C for 5 weeks to synchronize germination. Plates were brought into continuous light at ambient temperature for germination. Seedlings were transplanted into the soilless mix previously described, and the resulting M1 plants were grown in the greenhouse. More than 100 M1 plants were manually self-pollinated by gentle brushing with a small camel hair artist's brush or allowed to self-pollinate. At least 250 seeds from several fruit of each plant were harvested using the blender method

Received for publication 21 Oct 2022. Accepted for publication 14 Sep 2023.
Published online 8 Nov 2023.
We thank Sam Jones for help with the mutagenesis, and Jin Patrick Cho for help with maintaining plants.
Mention of a trademark, proprietary product, or vendor does not constitute a guarantee or warranty of the product by the US Department of Agriculture and does not imply its approval to the exclusion of other products or vendors that also may be suitable.
J.P. is the corresponding author. E-mail: janet.slovin@usda.gov.

(Morrow et al. 1954); then, they were dried and stored separately for each plant at 6 °C. Five seeds from each M1 plant that produced fruit were planted out, and the resultant M2 plants were screened for visually abnormal phenotypes over the course of the subsequent 3 years.

For observations of M2 plants, plants were manually selfed starting at flower opening and every day thereafter as their anthers dehisced until petal drop. To ensure adequate pollination, selfing was also performed with a brush dipped in pollen from anthers that were freshly dehisced in the presence of Drierite (calcium sulfate desiccant; W. A. Hammond Drierite, Co., Ltd., Xenia, OH, USA) in a 60- × 15-mm petri dish. Plants were crossed by removing anthers from the female parent with fine forceps immediately upon flower opening and manually pollinating with pollen from the male parent as described.

Filament length measurement. Filament lengths were determined using a Zeiss Discovery V12 to image groups of anthers dissected from just opened flowers with an AxioCam HRc camera. Measurements were performed using the Zeiss camera software.

Anther characterization. Plants were tested for the ability to dehisce and release pollen by removing individual anthers from the flower with fine forceps and placing them on double-sided tape in a small petri dish. Drierite desiccant was placed in the dish and the cover was replaced. The anthers were scored for pollen production 1 h later under a dissecting microscope.

For morphological evaluation, anthers were staged and processed according to Hollender et al. (2012). Buds were fixed in FAA (formaldehyde: ethanol: acetic acid: water, 10:50:5:35) and embedded in paraffin essentially as described by Hollender et al. (2012), except that Hemo De® (Scientific Safety Solvents, Keller, TX, USA) was used instead of xylene. Slides were stained with Safranin O and Fast Green as described by Hollender et al. (2012), except that Fast Green was dissolved in 95% ethanol/water and Hemo De® was used instead of xylene. Slides were examined under bright field using a Zeiss Axio Imager A.1 and photographed using a Zeiss AxioCam MRc5.

Results

Plant description. The M2 mutant plant EMS-T277 did not produce any berries or mature-appearing achenes (the true fruit of *Fragaria* spp. in the botanical sense) over a period of 3 years and was named *fruitless 1* (*ftl 1*). The mutant plants are smaller than, and not as robust as, wild-type (H4F7-3) (Fig. 1A). Like wild-type, *ftl 1* plants produce runners and can be clonally propagated from runners or by separating branch crowns. Unlike wild-type, leaves of the mutant are mottled, with mottling becoming more pronounced as the leaf ages (Fig. 1B and C). Bracts, sepals, and petals of the mutant flowers appear normal; however, the carpels and anthers are paler yellow than wild-type (Fig. 1D). The styles of the mutant appear thinner and disordered as compared with wild-type (Fig. 1D). The *ftl 1* anthers (Fig. 1G) are smaller than wild-type (Fig. 1F), and when dehisced in the laboratory, *ftl 1* anthers failed to show evidence of pollen grains (Fig. 1H), whereas wild-type anthers produced masses of clumped pollen (Fig. 1F).

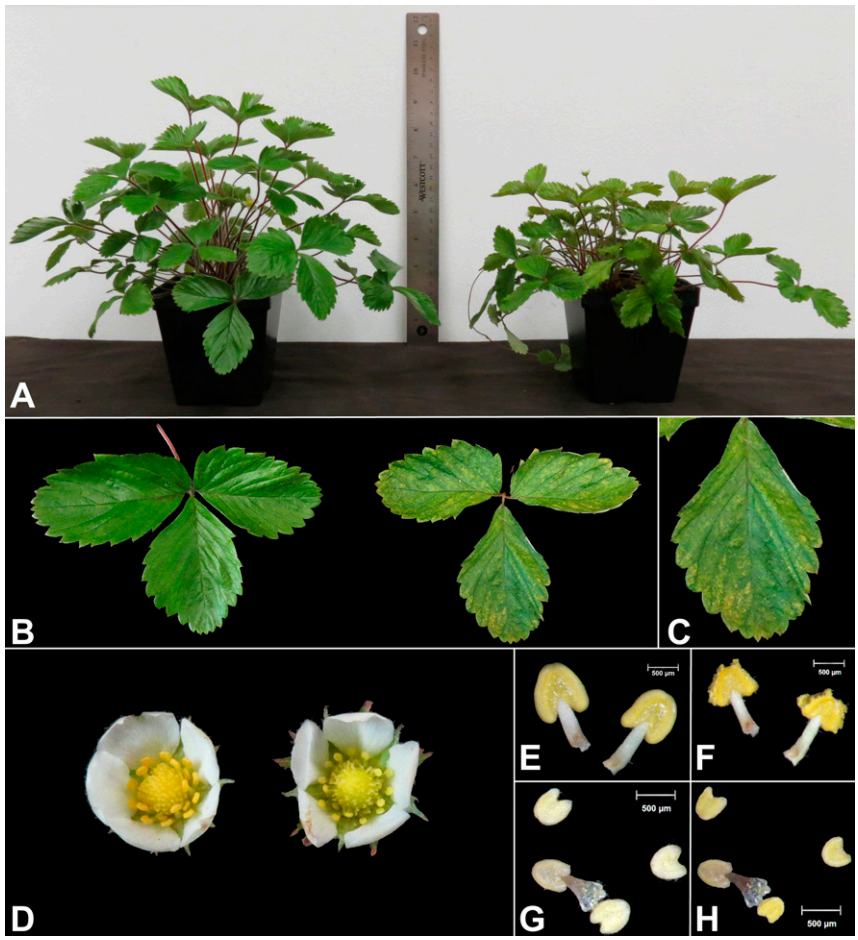

Fig. 1. Morphology and physiology of diploid strawberry Hawaii 4 (wild-type) and the *fruitless 1* mutant: (**A**) 6-month-old Hawaii 4 plants (left) and *fruitless 1* plants (right). The background ruler is 30 cm. (**B**) Hawaii 4 leaves (left) are larger than *fruitless 1* leaves (right). (**C**) Close-up of *fruitless 1* leaflet showing typical mottling seen on mutant leaves. (**D**) The *fruitless 1* flower (right) has paler carpels and anthers than the Hawaii 4 flower (left). (**E**) Hawaii 4 anthers before dehiscence; (**F**) Hawaii 4 anthers with pollen after dehiscence after 1-h incubation with desiccant. (**G**) The *fruitless 1* anthers before dehiscence. (**H**) The *fruitless 1* anthers after 1-h incubation with desiccant.

The mutant flowers have the same number of stamens as wild-type flowers, although the mutant filaments appear to be shorter (Fig. 1D). Figure 2A shows that *F. vesca* stamens are arranged in two whorls, with tall and short stamens in the inner whorl and medium-length stamens in an outer whorl (Hollender et al. 2012). A typical flower has five short and tall stamens and 10 medium-length stamens. The length of each stamen type varies from one flower to another and can vary within each individual flower; however, as seen in Fig. 2B, there are three distinct clusters of filament lengths in each of the four genotypes observed. Short *ftl 1* stamens or tall *ftl 1* stamens, whether from the parent mutant or the *ftl 1* phenotype F_2 progeny, are shorter than the corresponding stamens from wild-type plants (Fig. 2C).

Genetics. Like wild-type, *ftl 1* plants produce berries if manually pollinated with wild-type pollen. However, only two or three mature achenes containing seeds were found on each resulting *ftl 1* berry, whereas wild-type fruit showed greater than 50% fertilization using the same batch of H4F7-3 pollen. Fifteen seeds from this cross were planted out, and all F1 plants were wild-type. Seeds obtained by selfing one of the F1 plants were harvested, and 200 seeds were planted. Of these, 150 seeds germinated and 145 F_2 seedlings survived to the flowering stage. At least five anthers from each F_2 plant were scored for dehiscence and pollen production. The *ftl 1* phenotype was found for 26 of the 145 plants, indicating that *ftl 1* is most likely to result from mutation of a single gene (Table 1).

Anther and pollen development. Thin sections (10 µm) of H4F7-3 developing flower buds stained with safranin O and Fast green showed the same developmental morphology and staging (Fig. 3), as had been observed previously in a different inbred *F. vesca* line, Yellow Wonder 5AF7 (Hollender et al. 2012). At flower bud stage 8, the tapetum has already formed in the premeiotic anther (Fig. 3A and B) and appears as a ring of more densely staining purple or blue cells around the large microspore mother cells, which have prominent nuclei. In *ftl 1* anthers at stage 8, microspore mother cells

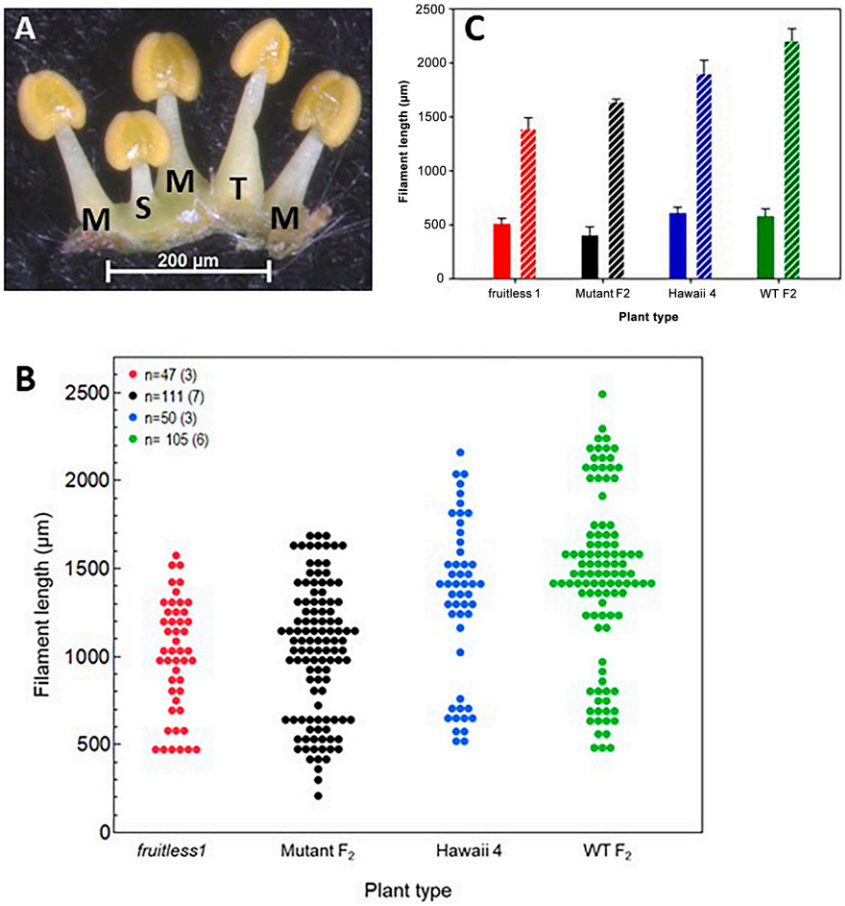

Fig. 2. The *fruitless 1* stamens are shorter than those of Hawaii 4 (wild-type). (**A**) Two whorls of stamens dissected from Hawaii 4 newly opened flowers illustrating the arrangement of the three sizes of stamens (M = medium; S = short; T = tall). (**B**) Distributions of stamen lengths from newly open flowers of wild-type (Hawaii 4), *fruitless 1*, F_2 plants with *fruitless 1* phenotype, and F_2 plants with wild-type phenotype. Each dot represents one stamen. The number of flowers observed is indicated in parentheses. (**C**) Average lengths of the short stamens (solid bars) and tall stamens (striped bars) using clustered data in (**B**).

have clearly formed and also have prominent nuclei with densely staining nucleoli. Unlike wild-type, there is not a clearly defined, blue, densely staining tapetal cell layer in *ftl 1* anthers at stage 8. The *ftl 1* slides were stained together with those of wild-type. Although the epithelial, endothelial, and middle cell layers surrounding the locule are evident, they are stained at the same density as the rest of the cells in the *ftl 1* anther lobe.

At flower bud stage 9, wild-type anthers are undergoing, or have undergone, meiosis and tetrads are visible in the locules (Fig. 3E and F). The wild-type tapetum is clearly defined by the blue staining, the angular cell shape, and the prominent nuclei. Cells that appeared somewhat like tetrads were visible in some of the stage 9 *ftl 1* anthers (Fig. 3H), although cellular disintegration, as seen in the both anthers in Fig. 3G and at the top of the anther in Fig. 3H, was evident in all *ftl 1* anthers observed at this stage.

In later-stage wild-type flower buds, the tapetum degenerates (Fig. 3I and J) and microspores, released from tetrads by the loss of callose, undergo mitotic divisions and develop into mature pollen grains by stage 12 (Fig. 3M and N). Anthers dehisce at stage 13. In contrast, cells in the locules of *ftl 1* anthers are clearly degenerating in stages 10 to 11 flower buds (Fig. 3K and L). Cells in the surrounding cell layers have become disorganized, and abnormal cell divisions can be seen in Fig. 3H. By stage 12, just before flower opening, locules of *ftl 1* have collapsed (Fig. 3O and P).

Table 1. The F_2 family resulting from a backcross of the diploid strawberry mutant *fruitless1* with wild-type, HI 4, as the male parent segregates ~3:1 (wild-type:*fruitless 1*), indicating that the phenotype is attributable to a recessive mutation in a single gene.

Phenotype	Expected	Observed	χ^2	*P*
Wild-type	109	119	0.917	
fruitless 1	36	26	2.778	
Total		145	3.697	0.05

Discussion

In strawberry, enlargement of the receptacle, which becomes the fleshy aromatic organ that is eaten, is dependent on fertilization of the carpels. The *F. vesca ftl 1* mutant was found among a population of M2 EMS mutant plants because none of its flowers exhibited receptacle enlargement, except when pollinated with wild-type pollen. Thus, the mutant was classified as male-sterile. Little is known about the process of anther and pollen development in strawberry; therefore, we further characterized *ftl 1* plants genetically and found that the *ftl 1* male-sterility most probably results from a recessive mutation in a single gene (Table 1). Because this mutation is EMS induced, it is likely to be a single nucleotide polymorphism or a small insertion/deletion. It remains to be determined whether the other phenotypic abnormalities of the *ftl 1* plants—the mottled leaf, the pale carpel and anther coloring, and the low female fertility—are pleiotropic effects of the *ftl 1* mutation or result from a cluster of EMS-induced mutations closely linked to *ftl 1*.

An anatomical comparison of *ftl 1* and wild-type anthers showed that *ftl 1* and wild-type anther development appear identical until flower stage 8 (anther stage 5 in Arabidopsis). For this study, stages of *F. vesca* anther development were defined based on characteristics of flower development such as petal morphology and developmental stage of carpels at the base and tip of the receptacle, as essentially described by Hollender et al. (2012). Microspore mother cells are evident in both *ftl 1* and wild-type anthers at flower stage 8, although the clearly defined and densely staining tapetum evident in wild-type is not seen in *ftl 1*. At flower stage 9, it is evident that *ftl 1* lacks tapetal cells, which stain distinctly with fast green in the wild-type. Tetrads are clearly seen in stage 9 wild-type anthers, whereas in *ftl 1* it appears that meiosis has been affected, and only a few tetrad-like structures are seen (Fig. 3E–H).

The tapetum is essential for development of the male gametophyte, both before meiosis and during pollen development (Marchant and Walbot 2022; Yao et al. 2022). In Arabidopsis, a critical role of the tapetum in early meiosis was recognized by an analysis of male-sterile plants with mutations in tapetum-expressed transcription factors DYSFUNCTIONAL TAPETUM (Zhang et al. 2006) and DEFECTIVE IN TAPETAL DEVELOPMENT (Zhu et al. 2008). Plants with mutations in another tapetum-expressed transcription factor, ABORTED MICROSPORES, develop normal-appearing tapetum and microspore mother cells (Ferguson et al. 2017; Xu et al. 2014). However, the *ams* plants fail to produce pollen because of abnormal cytokinesis during meiosis, with "irregular" tetrad formation and abnormal callose wall formation (Tidy et al. 2022). Like the *ams* mutants, the *ftl 1* anthers also produce microsporocytes that fail to undergo proper tetrad development, resulting in subsequent degeneration. Unlike *ams* mutants, *ftl 1* anthers do not appear to produce a normal tapetum, and it is not known how much tapetal function *ftl 1* anthers retain or at which stage meiosis is affected.

Tissue from members of the segregating F_2 population has been harvested for bulked sequence mapping of the mutated gene. Wild-type and mutant plants and the F1 seeds produced from backcrossing *fruitless 1* to H4F7-3 are available to the community for further collaborative research. Please contact Janet Slovin or the USDA-ARS National Clonal Germplasm Repository for materials.

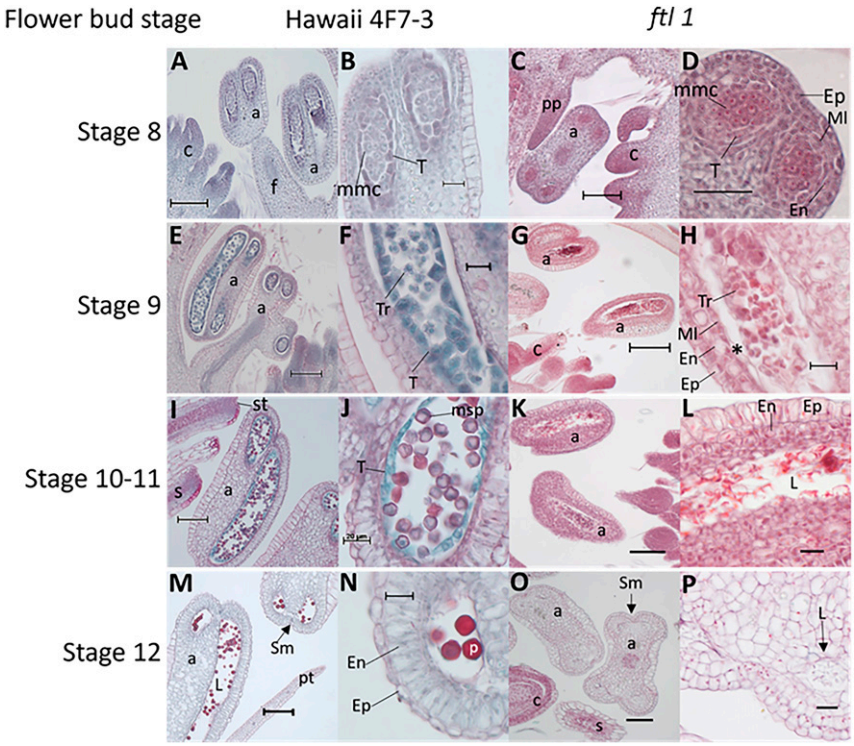

Fig. 3. Micrographs of anthers and carpels in paraffin-embedded sections of stages 8 through 12 flower buds from Hawaii 4 and *fruitless 1* plants. Bud stages are those described by Hollender et al. (2012). Sections (10 μm) were stained with Safranin O and Fast Green. Stage 8 Hawaii 4 (**A**, 20×; **B**, 40×). Stage 8 *fruitless 1* (**C**, 20×; **D**, 40×). Stage 9 Hawaii 4 (**E**, 20×; **F**, 40×). Stage 9 *fruitless 1* (**G**, 20×; **H**, 40×). Stages 10–11 Hawaii 4 (**I**, 20×; **J**, 40×). Stages 10–11 *fruitless 1* (**K**, 20×; **L**, 40×). Stage 12 Hawaii 4 (**M**, 20×; **N**, 40×). Stage 12 *fruitless 1* (**O**, 20×; **P**, 40×). * Abnormal cell division. a = anther; c = carpel; f = filament; En = endodermis; Ep = epidermis; L = locule; mmc = microspore mother cell; msp = microspore; p = pollen; pt = petal; s = style; st = stigma; T = tapetum; Tr = tetrad. Scale bar (**A**, **C**, **E**, **G**, **I**, **K**, **M**, **O**) = 100 μm. Scale bar (**D**) = 50 μm. Scale bar (**B**, **F**, **H**, **J**, **L**, **N**, **P**) = 20 μm.

References Cited

Brown T, Wareing PF. 1965. The genetic control of the everbearing habit and three other characters in varieties of *Fragaria vesca.* Euphytica. 14:97–112.

Cao S, Luo X, Xu D, Tian X, Song J, Xia X, Chu C, He Z. 2021. Genetic architecture underlying light and temperature mediated flowering in Arabidopsis, rice, and temperate cereals. New Phytol. 230:1731–1745. https://doi.org/10.1111/nph.17276.

Caruana JC, Sittmann JW, Wang W, Liu Z. 2018. *Suppressor of Runnerless* encodes a DELLA protein that controls runner formation for asexual reproduction in strawberry. Mol Plant. 11:230–233. https://doi.org/10.1016/j.molp.2017.11.001.

Duchesne N. 1766. Histoire Naturelle des Fraisiers. Didot Panckoucke, Paris, France.

Edger PP, Poorten TJ, VanBuren R, Hardigan MA, Colle M, McKain MR, Smith RD, Teresi SJ, Nelson ADL, Wai CM, Alger EI, Bird KA, Yocca AE, Pumplin N, Ou S, Ben-Zvi G, Brodt A, Baruch K, Swale T, Shiue L, Acharya CB, Cole GS, Mower JP, Childs KL, Jiang N, Lyons E, Freeling M, Puzey JR, Knapp SJ. 2019. Origin and evolution of the octoploid strawberry genome. Nat Genet. 51:541–547. https://doi.org/10.1038/s41588-019-0356-4.

Edger PP, VanBuren R, Colle M, Poorten TJ, Wai CM, Niederhuth CE, Alger EI, Ou S, Acharya CB, Wang J, Callow P, McKain MR, Shi J, Collier C, Xiong Z, Mower JP, Slovin JP, Hytönen T, Jiang N, Childs KL, Knapp SJ. 2018. Single-molecule sequencing and optical mapping yields an improved genome of woodland strawberry (*Fragaria vesca*) with chromosome-scale contiguity. Gigascience. 7:gix124–gix124. https://doi.org/10.1093/gigascience/gix124.

Feng J, Cheng L, Zhu Z, Yu F, Dai C, Liu Z, Guo W-W, Wu X-M, Kang C. 2021. GRAS transcription factor LOSS OF AXILLARY MERISTEMS is essential for stamen and runner formation in wild strawberry. Plant Physiol. 186:1970–1984. https://doi.org/10.1093/plphys/kiab184.

Ferguson AC, Pearce S, Band LR, Yang C, Ferjentsikova I, King J, Yuan Z, Zhang D, Wilson ZA. 2017. Biphasic regulation of the transcription factor ABORTED MICROSPORES (AMS) is essential for tapetum and pollen development in Arabidopsis. New Phytol. 213:778–790. https://doi.org/10.1111/nph.14200.

Guttridge CG. 1973. Stem elongation and runnering in the mutant strawberry, *Fragaria vesca* L. *arborea* Staudt. Euphytica. 22:357–361.

Hollender CA, Geretz AC, Slovin JP, Liu Z. 2012. Flower and early fruit development in a diploid strawberry, *Fragaria vesca.* Planta. 235:1123–1139. https://doi.org/10.1007/s00425-011-1562-1.

Kuo P, Da Ines O, Lambing C. 2021. Rewiring meiosis for crop improvement. Front Plant Sci. 12. https://doi.org/10.3389/fpls.2021.708948.

Li W, Zhang J, Sun H, Wang S, Chen K, Liu Y, Li H, Ma Y, Zhang Z. 2018. FveRGA1, encoding a DELLA protein, negatively regulates runner production in *Fragaria vesca.* Planta. 247:941–951. https://doi.org/10.1007/s00425-017-2839-9.

Luo H, Dai C, Li Y, Feng J, Liu Z, Kang C. 2018. *Reduced Anthocyanins in Petioles* codes for a GST anthocyanin transporter that is essential for the foliage and fruit coloration in strawberry. J Expt Bot. 69:2595–2608. https://doi.org/10.1093/jxb/ery096.

Marchant DB, Walbot V. 2022. Anther development—The long road to making pollen. Plant Cell. 12:4677–4695. https://doi.org/10.1093/plcell/koac287.

Morrow EB, Darrow GM, Scott DH. 1954. A quick method of cleaning berry seed for breeders. Proc Am Soc Hortic Sci. 63:265.

Pi M, Hu S, Cheng L, Zhong R, Cai Z, Liu Z, Yao JL, Kang C. 2021. The MADS-box gene FveSEP3 plays essential roles in flower organogenesis and fruit development in woodland strawberry. Hortic Res. 8:247. https://doi.org/10.1038/s41438-021-00673-1.

Rivarola M, Chan AP, Liebke DE, Melake-Berhan A, Quan H, Cheung F, Ouyang S, Folta KM, Slovin JP, Rabinowicz PD. 2011. Abiotic stress-related expressed sequence tags from the diploid strawberry *Fragaria vesca* f. semperflorens. Plant Genome. 4:12–23. https://doi.org/10.3835/plantgenome2010.08.0018.

Sargent DJ, Davis TM, Tobutt KR, Wilkinson MJ, Battey NH, Simpson DW. 2004. A genetic linkage map of microsatellite, gene-specific and morphological markers in diploid *Fragaria.* Theor Appl Genet. 109:1385–1391.

Slovin J, Rabinowicz PD. 2007. *Fragaria vesca*, a useful tool for Rosaceae genomics, p 112–117. In: Takeda F (ed). 6th North American Strawberry Symposium. American Society for Horticultural Science, Ventura, CA, USA.

Slovin J, Schmitt K, Folta K. 2009. An inbred line of the diploid strawberry Fragaria vesca f. semperflorens for genomic and molecular genetic studies in the Rosaceae. Plant Methods. 5:15.

Staudt G. 1959. Eine spontan aufgetretene Grossmutation bei Fragaria vesca L. Naturwissenschaften. 1:1–3.

Tenreira T, Lange MJP, Lange T, Bres C, Labadie M, Monfort A, Hernould M, Rothan C, Denoyes B. 2017. A specific gibberellin 20-oxidase dictates the flowering-runnering decision in diploid strawberry. Plant Cell. 29:2168–2182. https://doi.org/10.1105/tpc.16.00949.

Tidy AC, Ferjentsikova I, Vizcay-Barrena G, Liu B, Yin W, Higgins JD, Xu J, Zhang D, Geelen D, Wilson ZA. 2022. Sporophytic control of pollen meiotic progression is mediated by tapetum expression of ABORTED MICROSPORES. J Expt Bot. 73:5543–5558. https://doi.org/10.1093/jxb/erac225.

Wang S-m, Li W-j, Liu Y-x, Li H, Ma Y, Zhang Z-h. 2017. Comparative transcriptome analysis of shortened fruit mutant in woodland strawberry (*Fragaria vesca*) using RNA-Seq. J Integr Agric. 16:828–844. https://doi.org/10.1016/S2095-3119(16)61448-X.

Xu J, Ding Z, Vizcay-Barrena G, Shi J, Liang W, Yuan Z, Werck-Reichhart D, Schreiber L, Wilson ZA, Zhang D. 2014. ABORTED MICROSPORES acts as a master regulator of pollen wall formation in Arabidopsis. Plant Cell. 26:1544–1556. https://doi.org/10.1105/tpc.114.122986.

Yao X, Hu W, Yang Z-N. 2022. The contributions of sporophytic tapetum to pollen formation. Seed Biology. 1:1–13. https://doi.org/10.48130/SeedBio-2022-0005.

Zhang W, Sun Y, Timofejeva L, Chen C, Grossniklaus U, Ma H. 2006. Regulation of *Arabidopsis tapetum* development and function by DYSFUNCTIONAL TAPETUM1 (DYT1) encoding a putative bHLH transcription factor. Development. 133:3085–3095. https://doi.org/10.1242/dev.02463.

Zhu J, Chen H, Li H, Gao J-F, Jiang H, Wang C, Guan Y-F, Yang Z-N. 2008. *Defective in Tapetal Development and Function 1* is essential for anther development and tapetal function for microspore maturation in Arabidopsis. Plant J. 55:266–277.